Second International Conference on CFD in the Minerals and Process Industries
CSIRO, Melbourne, Australia
6-8 December 1999

A NUMERICAL AND EXPERIMENTAL STUDY OF TANGENTIALLY INJECTED SWIRLING PIPE FLOWS

Jiajun CHEN, Brian S. HAYNES and David F. FLETCHER

Department of Chemical Engineering, University of Sydney, NSW 2006, AUSTRALIA

ABSTRACT

Swirl flows induced by tangential inlets were studied using Computational Fluid Dynamics simulations (CFD) and experiments. The CFD simulations showed complex, steady, non-axisymmetric flow patterns for the three swirl flows of intermediate to low swirl intensity. It was found that the flow pattern was very sensitive to the initial swirl intensity. Axisymmetry was much easier to obtain in a higher swirl case with a swirl number of 0.8 than in lower swirl flows, with swirl numbers of 0.26 and 0.03. The computational results were found to be independent of the details of the inlet boundary conditions and equation solver method. However, a higher order convection scheme, such as the Van Leer scheme, needed to be used to capture the main flow features. In the experiments, a multi-hole pressure probe, called a Cobra probe, was used to measure the mean velocity profile. The results supported the existence of the calculated flow features.

NOMENCLATURE

A	Cross sectional area of the test section
A_j	Total cross sectional area of the tangential inlets
D	diameter of the test section
k	turbulence energy
M_T	total momentum flux through the test section
M_t	total momentum flux through the tangential inlets
m_T	total mass flowrate through the test section
m_t	total mass flowrate through the tangential inlets
R	radius of the test section
r	radial position
U	mean axial velocity
U_{av}	average axial velocity at a cross section
V	mean radial velocity
W	mean tangential velocity
x	axial position
ρ	density of air
Ω	local swirl intensity

INTRODUCTION

Swirling pipe flows have remained the subject of intensive experimental and numerical investigations. They are widely used in industrial devices, such as cyclone separators, combustion equipment and heat exchangers. Many studies on different types of confined swirl flows have been reported in the literature. The subject of this study is tangentially injected swirl flows. They are the simplest means of swirl generation among many others, such as the use of guide vanes and rotating parts. Their simplicity in geometry makes it possible to study the flow numerically without the need for detailed flow data on inlet conditions.

Previous studies of tangentially injected swirl flows have used a single tangential inlet or a pair/pairs of tangential inlets situated diametrically opposite each other. Symmetry was found for the flow induced by a pair of tangential inlets (Nissan and Bresan, 1961) and two and three pairs of tangential inlets (Chang and Dhir, 1994). In this study, swirl flows induced by a pair and two pairs of tangential inlets and an axial inlet were studied numerically using the CFX4 general purpose CFD code.

Different initial swirl intensities can be achieved by varying the air flowrate at the axial and tangential inlets. It was found that whether symmetry can be achieved depends on both the initial swirl intensity and the number of tangential inlets. The effects of different turbulence models, differencing schemes, linear equation solver methods and inlet conditions were also studied. Measurements of mean velocities were carried out using a four-hole pressure probe, called a Cobra probe, which has been validated in developed pipe flow (Chen, Fletcher and Haynes, 1998). The experimental data support the computational flow features simulated using CFX4.

NUMERICAL MODELLING

Model Description

Calculations have been performed for three cases with the same Reynolds number and different initial swirl intensities, achieved by setting 10%, 31% and 56% of the total flowrate at the tangential inlets. The Reynolds number based on the pipe diameter and the bulk velocity downstream of the swirler is about 10^5. A pair of tangential inlets has been used for all three cases. Additional calculations were performed using two pairs of tangential inlets for the medium swirl case with a swirl flowrate of 31%.

The geometry used for the calculations is shown in Figure 1. It consists of a cylindrical pipe of diameter 0.146m with a swirler of two or four tangential inlets inserted 1m downstream of the axial inlet and 9.7m upstream of the outlet. Details of the swirler are shown in Figure 2. The mesh, consisting of 87,420 cells, is illustrated in Figures 1 and 2. The cells are uniformly distributed at the cross section of the cylinder as shown in Figure 2. In the axial direction, the mesh is uniform and fine over the inlet region and is then stretched towards the exit. A mesh refinement study showed this to be fine enough to capture all the flow features. Coarsening the mesh by about 50% has the effect of increasing the decay rate slightly but altered none of the conclusions.

Two different turbulence models were used. The standard k-ε model (Wilcox, 1994) was applied in some calculations but most calculations used the differential Reynolds Stress model (DSM) (Launder *et al*, 1975) because of its superior treatment of swirl flows (Shore, Haynes, Fletcher and Sola, 1996).

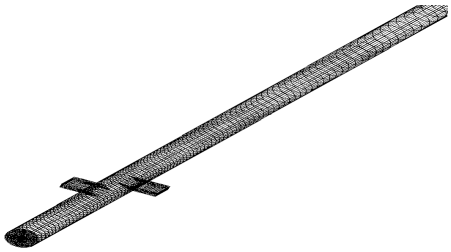

Figure 1: Geometry of the calculations for the two inlet swirler.

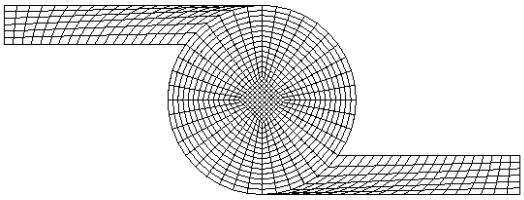

Figure 2: Details of the swirler geometry with two inlets.

Numerical Method

The governing equations can be found in Shore, Haynes, Fletcher and Sola (1996). The following boundary conditions were used unless otherwise stated. Uniform normal velocities were set at all inlets. The inlet turbulence levels were set to that for fully developed pipe flow. Uniform pressure was set at the outlet. All walls were assumed to be smooth, and standard log-law wall functions were applied.

The system of equations and boundary conditions was solved using a finite volume method on a non-staggered grid, coded in CFX4 (CFX, 1997). Mass conservation is obtained using the SIMPLEC method with the Rhie-Chow algorithm.

A previous study (Shore, Haynes, Fletcher and Sola, 1996) indicated that the Van Leer scheme (Van Leer, 1977) and the QUICK scheme (Leonard, 1979) are superior to other schemes for swirl flows of this type. Therefore in this study, the convection scheme of Van Leer was used for all the calculations unless otherwise indicated. The resulting algebraic equations were solved using an algebraic multigrid method for pressure and velocities and line relaxation for all other variables. Under relaxation and false time stepping were used for various runs. For the highest swirl flow, an under-relaxation factor of 0.7 was used for the pressure, and false timesteps of 0.001s were used on the velocities and the turbulence variables. For the medium swirl case, false timesteps of 0.01s were used for the DSM calculations. For the other runs, default under-relaxation factors of 0.7 were used for velocities and 0.4 for turbulence variables.

EXPERIMENTAL STUDY

Experimental Set-up

The experimental rig used in the present study has been altered from a previous set-up for the study of pipe flow (Chen, Fletcher and Haynes, 1998). Basically, it consists of an inlet section, test section, flowmeter, baffle box and a variable speed fan. In the inlet section, a conical contraction, a tube bundle flow straightener and two mesh screens were installed upstream of the swirler. This set-up produced a fairly uniform velocity distribution at the axial opening of the swirler. Smooth aluminum tubing with a diameter of 0.146m was used as the test section. After the test section, a Mitsubishi flow conditioner (Miller, 1983) was inserted into the pipe. It helps to remove the swirl and the distortion of the velocity profile and to produce a fully developed flow profile for the vortex flowmeter situated 22D downstream of the conditioner. The flowrates at the tangential inlets and the axial inlet were adjusted by means of fine cloths covering the openings. The flowrate at the axial inlet was determined by measuring the pressure drop at the tube bundle flow straightener. A predetermined calibration curve, obtained using pure axial flow and the vortex flowmeter, was used to correlate the pressure drop with the flowrate. This method is simple, yet effective, and it avoided extra pipe setting and a second flowmeter.

Measurement Procedure

The flowfield behind the swirler was measured using a four-hole pressure probe, called a Cobra probe. The probe has been validated in a developed pipe flow, in which it showed good agreement with well documented hot-wire data (Chen, Fletcher and Haynes, 1998).

The Cobra probe can measure the total velocity, flow direction and static pressure, as well as the Reynolds stress terms. Details of its principle can be found in the literature (Musgrove and Hooper, 1993). Generally, the probe is able to resolve flows at a relative angle of up to 45° to the probe head. In this application the direction of the swirl flow is unknown. Therefore, a mechanism was used to rotate the probe about its axis at a certain interval while fixing its head in the same position. An optimum position, which is the nearest position to the flow direction, was then found by utilizing the structure of the probe head. In this study, it was achieved by comparing the pressures of the centre hole and the two symmetrical holes registered by the probe at various positions. This method is found to be more effective than the previous method (Musgrove and Hooper, 1993), which used only the centre hole pressure.

NUMERICAL RESULTS

Effects of Initial Swirl Intensity

Steady state calculations were carried out for flows of different initial swirl intensities induced by swirlers with two tangential inlets. The DSM and the Van Leer differencing scheme were used. Three different initial swirl intensities were obtained by setting the proportion of the air entering the two tangential inlets to the total flowrate to 56%, 31% and 10% with equal flowrate at the two tangential inlets.

The local swirl intensity, Ω, the ratio of the axial flux of tangential momentum to the axial flux of axial momentum at a cross section, can be defined as

$$\Omega = \frac{2\pi\rho\int_0^R UWrdr}{\rho\pi R^2 U_{av}^2} \qquad (1)$$

where U_{av}, U and W are the bulk axial velocity, the mean axial velocity and the mean swirl velocity, respectively, R is the pipe radius and ρ is the air density (Chang and Dhir, 1994). Another important parameter is the ratio of the momentum flux through the tangential inlets to the total momentum flux through the test section, defined as

$$\frac{M_t}{M_T} = \frac{m_t^2}{m_T^2}\frac{A}{A_j} \qquad (2)$$

where m_t and m_T are the total mass flowrates through the tangential inlets and the test section, respectively. A and A_j are the cross sectional area of the test section and the total area of the tangential inlets, respectively. As indicated by Chang and Dhir, at the swirler location the local swirl intensity should be equal to the ratio M_t/M_T due to conservation of momentum. According to Equation (2), the initial swirl intensities of the three flows in this study are 0.8, 0.26 and 0.03.

The contour plots of axial velocity at different axial positions for the three flows are shown in Figure 3. As expected from the geometry and inlet conditions, symmetry can be found for a diametral line at any azimuthal position for all the flows. It is also true for the radial and tangential velocities, although they are not shown here. However, the flows were generally non-axisymmetric. Figure 4, giving the axial, radial and tangential velocity distribution along two lines parallel to and about 0.8R away from the pipe axis, exhibits the non-axisymmetry quantitatively. As the two lines are 90° apart (one is in the plane parallel and the other is in the plane perpendicular to the tangential inlets), they give the range of maximum difference in azimuthal positions.

One expects non-axisymmetry to exist in the region immediately after the non-axisymmetric swirler, and then to decrease and die out as mixing progresses downstream. From Figures 3 and 4, it can be seen that this is generally true for the flows calculated. However the degree of the non-axisymmetry and its decay are very different for flows of different initial swirl intensities.

The degree of axisymmetry of the high swirl case is much higher than the medium and low swirl cases, but the low swirl case is better than the medium swirl case. One interesting phenomenon found was that for the high and medium swirl cases the magnitude of the three velocity components along the two lines was oscillating. For the radial velocity this was accompanied by changes of direction. This velocity oscillation was most apparent near the swirler, then it decreased further downstream as the degree of axisymmetry increased. For the high swirl case, a distance of about 10D is needed to obtain approximate axisymmetry. For the medium swirl case, the oscillation appeared at a much higher magnitude and remained throughout the whole computational domain of about 65D.

For the very low swirl case, non-axisymmetric flow was only evident for the axial velocity, as the radial and tangential velocities are very low. There was no oscillation of the velocity magnitude in space and approximate axisymmetry can be observed at about 14D downstream of the swirler.

Close examination of the flowfield showed that the oscillation of the velocity magnitude and direction in the axial direction is caused by a vortex wound about the axis of the pipe. However, the shape of the vortex differs at different swirl intensities, due to the interaction between the axial inflow and the tangential jets, shown in Figure 3. Generally, the effect of the tangential jets is to impose a hydrodynamic contraction on the axial inflow and to cause the axial velocity to increase near the pipe centre. In the low and the medium swirl cases, this contraction only affected part of the axial inflow, depending on how far the tangential jets penetrate in the azimuthal direction. The non-axisymmetry and the velocity oscillation in space correspond to the parts of the flow that were affected and not affected by the contraction. The higher the swirl the higher the degree of no-axisymmetry, until the swirl is high enough that a complete 'roll-up' occurs, as in the high swirl case in this study. In this case the contraction is imposed on almost the whole axial inflow and a symmetric swirl flow is established soon after injection.

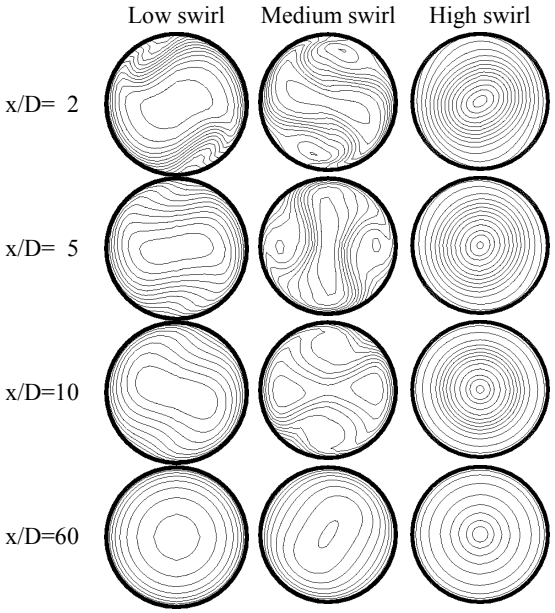

Figure 3: Calculated mean axial velocity contour at different axial positions for three flows of different initial swirl intensities induced by the swirler with two tangential inlets.

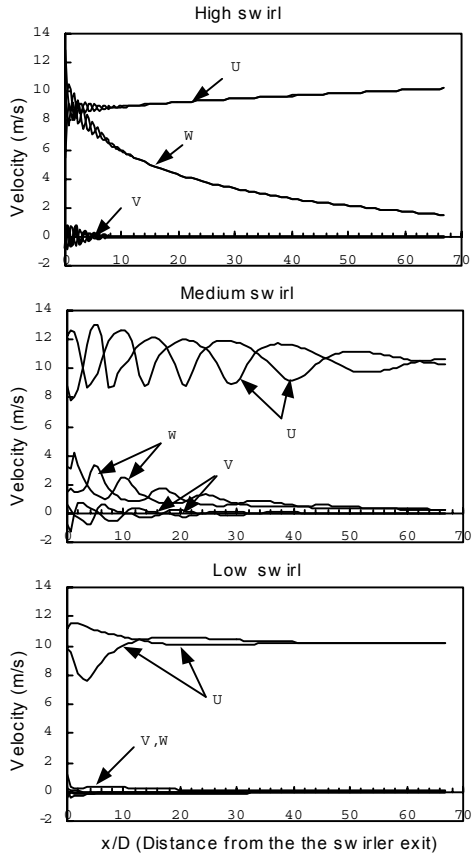

Figure 4: Calculated U, V and W velocity for three swirl flows induced by two tangential inlets. The data are for the flows at two lines parallel to and 0.8R away from the pipe centre line. The calculations used the DSM with Van Leer differencing.

Effect of the Turbulence Model and Convection Scheme

Calculations were performed for the medium swirl flow case using the k-ε model and the DSM, both with the Van Leer differencing scheme. Figure 5 shows the velocity at two lines that are parallel to the pipe axis but 90° apart for the two calculations. These show that the phenomenon of non-axisymmetry and velocity oscillation was reproduced by the k-ε model, but with a slightly faster decay.

The effect of convection schemes was studied for the medium swirl flow using the k-ε model. Here the Van Leer and a lower order scheme, the Upwind scheme, were used for comparison. The results, presented in Figure 6, indicated that the Upwind scheme predicted a much quicker decay of the non-axisymmetry and the velocity oscillation than the Van Leer scheme did, while giving a similar initial non-axisymmetry. These results are consistent with a previous study (Shore, Haynes, Fletcher and Sola, 1996), where it was found that the k-ε model is more diffusive than the DSM, and that the lower order differencing schemes, such as Upwind, produced excessive numerical diffusion compared with higher order schemes, such as the Van Leer and QUICK schemes.

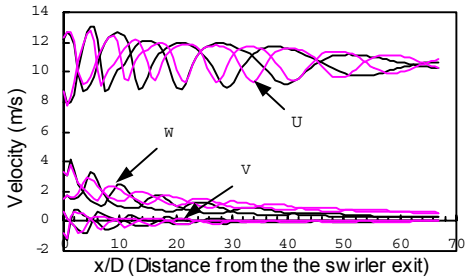

Figure 5: Calculated U, V and W velocity for the medium swirl induced by two tangential inlets. The data are for flows at two lines parallel to and 0.8R away from the pipe centre line. The calculations used the k-ε model or the DSM with the Van Leer differencing scheme (dark lines: DSM, grey lines: k-ε).

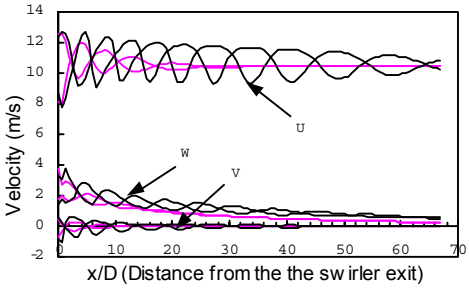

Figure 6: Calculated U, V and W velocity for the medium swirl induced by two tangential inlets. The data are for flows at two lines parallel to and 0.8R away from the pipe centre line. The calculations used the k-ε model with the Van Leer or the Upwind schemes (dark lines: Van Leer, grey lines: Upwind).

Effect of the Equation Solving Method

A calculation was performed using a coupled solver based on an additive correction multigrid method (Hutchinson, Galpin and Raithby, 1988) for the linear equations, which is implemented in the CFD package CFX-TASCflow (CFX, 1999). Here the k-ε model and a higher order differencing scheme (second order Upwind with a physical advection correction) of equivalent accuracy to the Van Leer scheme were used. The result was very similar to the results using the iterative method with the k-ε model and Van Leer differencing in CFX4. This showed that the predicted behaviour is not a function of the segregated solver used in CFX4.

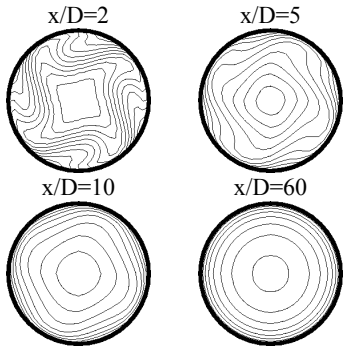

Figure 7: Calculated mean axial velocity contour at different axial positions for the medium swirl flow case induced by four tangential inlets.

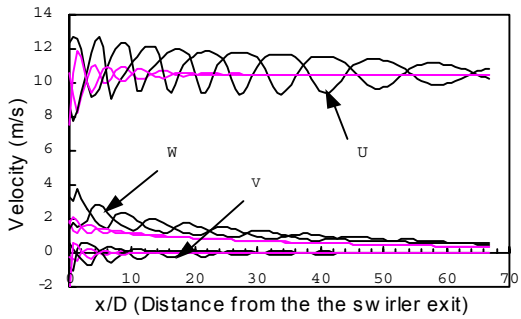

Figure 8: Calculated U, V and W velocity for the medium swirl induced by two and four tangential inlets. The data are for the flow at two lines parallel to and 0.8R away from the pipe centre line. The calculations used the k-ε model and the Van Leer differencing scheme (dark line: two inlets, grey lines: four inlets).

Effect of the Number of Tangential Inlets

The effect of the number of tangential inlets was investigated by comparing the flowfield behind the swirler for two and four evenly spaced tangential inlets for the medium swirl flow case. Here the total swirl flowrate was kept at 31% of the total flowrate, and the k-ε model and the Van Leer differencing scheme were used in CFX4. As expected, the flowfield resulting from four tangential inlets is much more uniform than that resulting from two tangential inlets, as shown in Figures 7 and 8.

In Figure 8, the velocity distribution along two lines parallel to and about 0.8R away from the axis were used for comparison. The two lines are 90° and 45° apart for the flow induced by two and four tangential inlets, respectively. Approximate axisymmetry can be observed at about 25D downstream of the swirler for the four tangential inlets case. This is a much shorter distance than that for the flow with the same swirl intensity but induced by two tangential inlets. However, it is still longer than that for the flow of high swirl intensity induced by two tangential inlets.

EXPERIMENTAL RESULTS

Experiments were carried out for the high and medium swirl flows induced by two tangential inlets. The mean velocity distributions at different axial positions ranging from 2D to 35D downstream of the swirler are presented in Figure 9 and 10 for the two cases, respectively. All the measurements were taken on a diametral line parallel to the tangential inlets. Comparisons were made with the computational results using the DSM and the Van Leer differencing scheme.

In Figure 9, gradual decay of the swirl and radial velocity is shown for the high swirl flow. Good symmetry was found on the diametral lines, and no flow pattern change was found at different axial locations. In the calculation, the axial velocity showed a peak at the centre line, while the experimental data showed a more developed profile. Good agreement between the calculated and measured swirl velocities at about 4D downstream of the swirler was found. However, at about 35D downstream of the swirler, the calculation predicted a combined type of swirl flow with a small forced vortex core, a large annular free vortex and a transition region between them, whilst the measured data showed a profile very close to a forced vortex flow. The calculation also underpredicted the radial velocity.

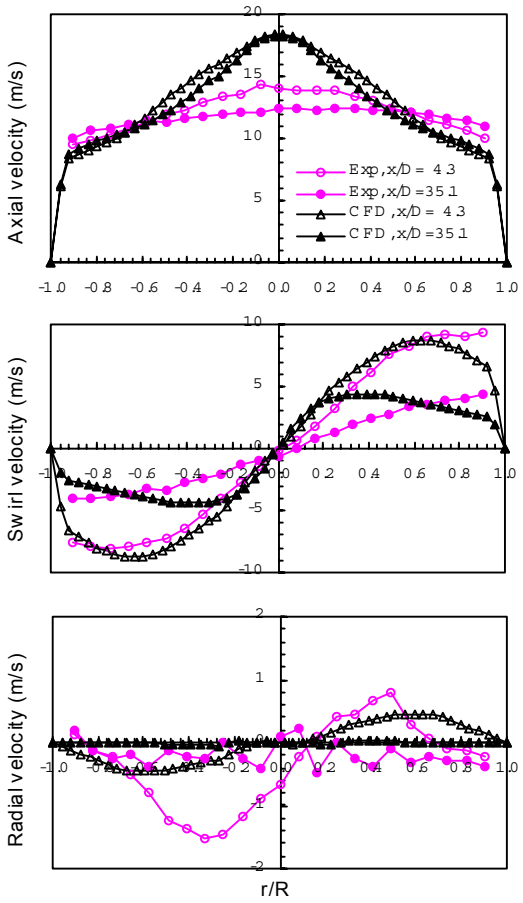

Figure 9: Measured and calculated mean velocities at different axial locations for the high swirl case.

Figure 10, which shows the flow data for the medium swirl case, indicates that the symmetry on the diametral line is not always present. Changes of flow pattern at different axial positions are evident from the axial velocity profile and the change of the radial velocity sign, as predicted by the calculation. Agreement between the calculation and the experiments is however only qualitative.

The calculated axial velocity profile at certain locations appears to be entirely below that at an upstream location, e.g. at x/D=2.2. However, close examination showed that at these locations the velocity values were higher near the wall. This also explains the same features found in the experimental data.

The current experimental data are preliminary in nature and clearly exhibit some limitation, for example, the zero shifts in the radial velocity shown in Figure 10. However, they do show a clear difference between the behaviour at high and medium swirl, as predicted in the simulations, despite the fact that the detailed profiles differ between the experiments and the computations. Further work is underway to investigate these differences.

Several studies on tangentially injected swirl flows have been reported in the literature. Nissan and Bresan (1961) studied the flows induced by a swirler with two tangential

inlets and no axial opening. The resulting swirl was very strong with an initial swirl number of 8.0 (calculated according to Equation (2)) and Reynolds number ranging from 5,000 to 25,000. Symmetry was found throughout the cylinder (6D to 42D). Chang and Dhir (1994) investigated the swirl flows induced by swirlers with four and six tangential inlets and no axial opening. The flows had initial swirl numbers of 2.67 and 7.84, with a Reynolds number of 12,500. No asymmetry was reported for the flows at 6D to 10D away from the swirler. This is consistent with our observation that it is easier to obtain axisymmetry in a flow of high swirl intensity.

CONCLUSIONS

CFD simulations have been performed to study the flowfield downstream of a tangential inlet swirler for swirl numbers in the range 0.03 to 0.8. The results are well converged and independent of the details of the inlet conditions. It is found that the flowfield behind a tangential inlet swirler is strongly dependent on the proportion of flow entering the tangential inlets to the total flowrate, i.e. the initial swirl intensity, but also dependent on the number of tangential inlets. Complex three-dimensional flow behaviour was found behind the swirler for all of the three swirl flows, which decayed more or less far downstream. They showed that it is easier to obtain an axisymmetric flowfield in a strongly swirling flow of swirl number 0.8 than in an intermediate swirl flow of swirl number 0.26. In the experiments, the changing of flow pattern at different axial locations is evident in the medium swirl case but was not observed in the high swirl case. The experiments revealed some qualitatively similar flow features and some features that are very different. The need for more detailed experimental data is clear, and this will form part of our future work.

ACKNOWLEDGEMENTS

This work was funded by a SPIRT grant in collaboration with BHP Research and TFI.

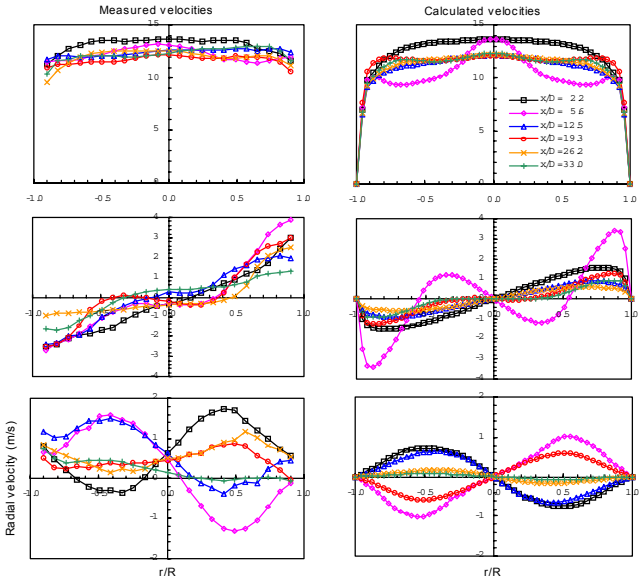

Figure 10: Measured and calculated mean velocities at different axial locations for the medium swirl case.

REFERENCES

CFX, (1997), "CFX-4.2: Solver Manual", CFX International, Harwell, Didcot, Oxfordshire, UK.

CFX, (1999), "CFX-TASCflow Solver Manual", CFX Int., Waterloo, Canada.

CHANG, F. and DHIR, V. K., (1994), "Turbulent flow field in tangentially injected swirl flows in tubes", Int. *J. Heat and Fluid Flow*, **15**, 5, 346-356.

CHEN, J., FLETCHER, D. F. and HAYNES, B. S., (1998), "Validation of the cobra probe using turbulence measurements in a fully developed pipe flow", *Proc. 13th Australisian Fluid Mech. Conf.*, 385-388, Monash University, Melbourne, Australia, December 13-18.

Hutchinson, B. R., Galpin, P. G. and Raithby, G. D., (1988), "Application of Additive correction multigrid to the coupled fluid flow equations", *Numerical Heat transfer*, **13**,133-147.

Launder, B. E., Reece, G. J. and Rodi, W., (1975), Progress in the development of a Reynolds stress turbulence closure, J Fluid Mech., **68**(3), 537-566.

Leonard, B. P, (1979), "A stable and accurate convective modelling procedure based on quadratic upstream interpolation", *Comp. Math. Appl. Mech. Engg*, **9**, 59-98.

MILLER, R. W., (1983), "Flow measurement engineering hand book", McGraw-Hill.

MUSGROVE, A. R. and HOOPER, J. D., (1993), "Pressure probe measurement of the turbulent stress distribution in a swirling jet", *Proc. 3rd World Conf. on Exp. Heat Transfer, Fluid Mech. and Thermodynamics*, 172-179, Hawaii, USA, October 31- November 5.

NISSAN, A. H. and BRESAN, V. P., (1961), "Swirling flow in cylinders", *A.I.Ch.E. Journal*, **7**, 4, 543-547.

SHORE, N. A., HAYNES, B. S., FLETCHER D. F. and SOLA, A. A., (1996), "Numerical aspects of swirl flow computation", *Proc. CTAC95*, 693-700, Melbourne, Australia, July 3-5, 1995.

Van Leer, B., (1977), "Towards the ultimate convection difference scheme, IV, A new approach to numerical convection", *J Comp. Phys*., **23**, 276-299.

Wilcox, D. C., (1994), "Turbulence modelling For CFD", DCW Industries Inc.